frontiers in Earth Science

ORIGINAL RESEARCH
published: 28 January 2022
doi: 10.3389/feart.2021.795519

Sedimentary Anthropogenic Carbon Signals From the Western Pacific Margin for the Last Century

Jay Lee[1†], Rick J. Yang[1†], Hui-Ling Lin[1], Yi-Chi Chen[2], Ren-Yi Cai-Li[2], Haojia Ren[2,3] and James T. Liu[1]*

[1]Department of Oceanography, National Sun Yat-sen University, Kaohsiung, Taiwan, [2]Department of Geosciences, National Taiwan University, Taipei, Taiwan, [3]Research Center for Future Earth, National Taiwan University, Taipei, Taiwan

The declining trend of the $\delta^{13}C$ of tropical corals over the last century was about –0.01‰ $year^{-1}$, according to global coral records. The decrease was attributable to the significant input of anthropogenic CO_2 (^{13}C Suess effect) to the atmosphere. Previous studies of $\delta^{13}C$ in corals suggested that the signal of the anthropogenic carbon in the Pacific and Indian Oceans were weaker than that in the Atlantic Ocean. However, biases relating to environments in which corals grew caused concerns. To investigate the anthropogenic carbon signal in the Western Pacific, foraminiferal records in a suite of 13 box cores with good age control were obtained from the continental slope off southwestern Taiwan between 2004 and 2006. $\delta^{18}O$ values of planktonic foraminifera (*Globigerinoides sacculifer* or so-called *Trilobatus sacculifer*) in collected cores were relatively stable at –2.5‰ to –2‰ in the last century, but foraminiferal $\delta^{13}C$ had a gradual secular decline after the 1900s. The decline trend of $\delta^{13}C$ began to intensify after the 1960s, and its rate was similar to that observed in the Atlantic. Similar decline trends of $\delta^{13}C$ were also found in coral records at regions where the human activity is high (Liuqiu) and low (Dongsha). Our findings indicate that the anthropogenic carbon signal in the Western Pacific was not weaker than that recorded in the Atlantic, and the nearshore sediment can supplement the lack of $\delta^{13}C$ records in corals, which are deficient when the environment is not suitable to grow.

Keywords: anthropogenic activity, corals, sediment cores, $\delta^{13}C$, $\delta^{18}O$, foraminifera

OPEN ACCESS

Edited by:
Daidu Fan,
Tongji University, China

Reviewed by:
Xuefei Chen,
Guangzhou Institute of Geochemistry (CAS), China
Jeroen Groeneveld,
University of Hamburg, Germany
Sui Wan,
South China Sea Institute of Oceanology (CAS), China

****Correspondence:***
Hui-Ling Lin
hllin@mail.nsysu.edu.tw

[†]These authors have contributed equally to this work and share first authorship

Specialty section:
This article was submitted to Marine Geoscience, a section of the journal Frontiers in Earth Science

Received: *15 October 2021*
Accepted: *14 December 2021*
Published: *28 January 2022*

Citation:
Lee J, Yang RJ, Lin H-L, Chen Y-C, Cai-Li R-Y, Ren H and Liu JT (2022) Sedimentary Anthropogenic Carbon Signals From the Western Pacific Margin for the Last Century. Front. Earth Sci. 9:795519. doi: 10.3389/feart.2021.795519

INTRODUCTION

Large quantities of CO_2 have been emitted into the atmosphere since the late 18th century as a result of human activities like fossil fuel burning, deforestation, and cement manufacturing (Crutzen and Stoermer, 2000). The input of the anthropogenic carbon not only altered lateral carbon fluxes from the land to the ocean but also influenced the climate on continental scales (Khatiwala et al., 2009; Höök and Tang, 2013; Regnier et al., 2013; Hansen and Stone, 2016).

The pathway of anthropogenic CO_2 entering the ocean is through gas exchanges across the air–sea interface (Suess, 1955; Keeling, 1979; Broecker and Maier-Reimer, 1992; Quay et al., 1992). The perturbation of carbon fluxes from the land to the ocean was calculated to be about 1.0 PgC $year^{-1}$ since the Industrial Revolution (Regnier et al., 2013), and the uptake of anthropogenic CO_2 by oceans was estimated up to 70% on the time scales of thousands of years (Archer et al., 1998; Raven and Falkowski, 1999). However, the current oceanic capacity only accounts for around one-third of the value because of the slow mixing rate (Field and Raupach,

2004; Sabine et al., 2004). Approximately 30% of the anthropogenic CO_2 was found at water depths shallower than 200 m (Sabine et al., 2004).

The penetration and distribution of the anthropogenic CO_2 concentration in oceans have been investigated by various instruments and proxies, among which carbon isotopes in sedimentary records are conventionally applied (Sabine et al., 2004; Khatiwala et al., 2009; Höök and Tang, 2013; Regnier et al., 2013). Fossil fuels stored in geological reservoirs contain high ^{12}C (lighter carbon isotope than ^{13}C) because the buried C3 plants discriminated against ^{13}C in the photosynthesis occurring hundreds of millions to tens of millions of years ago (Farquhar et al., 1989; Graven et al., 2020). As a result, the combustion of fossil fuels releases the lighter carbon isotope and causes the ^{12}C concentration to increase faster than ^{13}C in the atmosphere. Consequently, the carbon isotopic composition of ^{13}C ($\delta^{13}C$: the ratio of $^{13}C/^{12}C$) depletes both in atmospheric and oceanic environments. The ^{13}C depletion associated with anthropogenic combustions, which induce CO_2 emission, is signified as the Suess effect (Keeling, 1979).

The ^{13}C Suess effect is not only archived in the atmosphere (Suess, 1955; Friedli et al., 1986) but also imprinted in marine realms (Quay et al., 1992; Swart et al., 2010; Black et al., 2011; Mellon et al., 2019; Simon et al., 2020). The significant decline trend of the $\delta^{13}C$ was measured in corals or sclerosponges pervasively distributed over the Atlantic, Indian, and Pacific Oceans (Damon et al., 1978; Nozaki et al., 1978; Druffel and Benavides, 1986; Wei et al., 2009; Swart et al., 2010). The decline rate of the $\delta^{13}C$ in the Atlantic Ocean was found to be greater than that in the Indian and the Pacific Oceans because of physiological activities of corals, local bathymetric conditions, or different buffer capacities in marine regimes (Takahashi et al., 1993; Sabine et al., 2004; Swart et al., 2010). Therefore, there are constraints to demonstrate the temporal variability of stable carbon isotopes by using coral records.

The calcium carbonate deposits in marine sediments (e.g., foraminifera) are regarded as another potential research material due to the wide coverage without constraints (e.g., water depth, turbidity; Mcconnaughey, 1989; Grottoli and Wellington, 1999; Linsley et al., 2019). The foraminiferal $\delta^{13}C$ records are often used to extract the environmental and metabolic information, though the offset exists because of physical and biogeological processes (Spero and Williams, 1988; Jonkers et al., 2013; Gaskell and Hull, 2019). For example, the fossil benthic foraminifera had indicated the negative excursion of the long-term $\delta^{13}C$ variability occurring within this century, which was related to the anthropogenic CO_2 emission (Al-Rousan et al., 2004; Mellon et al., 2019).

In addition to carbon isotopes, the composition of oxygen isotopes ($\delta^{18}O$: the ratio of $^{18}O/^{16}O$) in the foraminiferal shell are widely used to estimate changes in the water temperature or glacier volumes (Shackleton, 1967; Thunell et al., 1999). In tropical and subtropical oceans, $\delta^{18}O$ records in foraminifera and corals have been applied to reconstruct the history of the sea surface temperature and the sea surface salinity over the century scale (Qiu et al., 2014; Watanabe et al., 2014; Raza et al., 2017). The foraminiferal $\delta^{18}O$ is also conventionally used to reflect the $\delta^{18}O$ in the ambient seawater (Katz et al., 2010). Tao et al. (2013) indicated that the varying $\delta^{18}O$ represented variabilities in hydrographic conditions such as the strength of the local upwelling and the freshwater input.

However, related studies are few due to low resolutions inhibited by the sedimentation rate in the open ocean. Furthermore, the near-shore realm with high sediment rates is usually intrigued by bioturbations, which can only be exempted in anoxic bottom conditions (Schimmelmann et al., 1990; Kennedy and Brassell, 1992; Black et al., 2007; Black et al., 2011). Therefore, the isotopic signal in sediments is crucial to be further studied. A suite of short box cores was collected from the continental slope off southwestern Taiwan in this study. Downcore sediment records were constrained by fallout radionuclides including ^{210}Pb and ^{137}Cs. The activity of radionuclides shows fairly constant hemipelagic accumulations and indicates that the near-shore realm was stable with high sedimentation rates. Therefore, our sediment cores provide good quality records in $\delta^{13}C$ and $\delta^{18}O$ to compare with coral isotope records collected in different areas such as Liuqiu and Dongsha. Liuqiu is located near our sampling sites, and Dongsha is around 424 km away from sampling sites in the northern South China Sea (SCS). Such precious materials provide insight information regarding the anthropogenic imprint in the Western Pacific for the last century.

MATERIALS AND METHODS

Sediment cores

FATES (Fate of Terrestrial/Nonterrestrial Sediments) Program was conducted to understand processes and responses of substances from the land to the marine sink. A suite of 13 short box cores were collected between 2004 and 2006 from the continental slope off SW Taiwan, northern SCS (**Table 1**; (Huh et al., 2009; Liu et al., 2009). Locations of sediment cores are shown on the bathymetric map (**Figure 1**), and information regarding geographic coordinates, water depths, and core lengths are listed in **Table 1**. Sediments were sampled at 5-cm intervals throughout sediment cores for foraminiferal isotope analyses. Planktonic shell sizes used for isotopic measurements were constrained by the sieving mash size of 300–355 μm for *Globigerinoides sacculifer* (so-called *Trilobatus sacculifer*) to minimize ontogenetic effects. Benthic foraminiferal shells of *Uvigerina* sp. were picked from a fraction greater than 150 μm. Stable isotopic analyses were done on groups of 10 specimens or less for each sample. The picked foraminiferal specimens were cleaned thoroughly in an ultrasonic bath with methanol to remove adhering fine particles, followed by soaking in sodium hypochlorite (NaOCl, 5%) at room temperature for more than 24 h to further remove any fine organic particles. Cleaning with deionized distilled water followed, and samples were then oven dried at 50°C. Stable isotope analyses for specimens were measured at the Stable Isotope Laboratory, National Taiwan University, Taiwan, following standard procedures with a precision better than 0.07‰ for $\delta^{18}O$ and 0.04‰ for $\delta^{13}C$.

TABLE 1 | The information of coring sites.

	Samples from sediment cores			
	Latitude (°N)	**Longitude (°E)**	**Depth (m)**	**Length of the core (cm)**
Collected in October 2004				
732-27B	22.19	120.26	825	48
Collected in December 2005				
779-St9	22.38	120.23	302	42
779-St11	22.29	120.14	767	36
Collected in April 2006				
789-L1	22.05	120.23	911	26
789-L9	22.18	120.36	491	50
789-L10	22.20	120.30	662	32
789-L11	22.23	120.26	721	38
791-K38	22.04	120.02	1,261	36
791-L26	22.40	120.22	307	40
791-L29	22.42	120.08	638	40
791-L30	22.37	120.13	683	34
791-L32	22.34	120.09	732	46
791-X1	22.22	120.38	376	42
Samples from coral				
Collected in June 2017				
Liuqiu	22.35	120.36	10	
Collected in June 2013				
Dongsha	20.67	116.83	2	

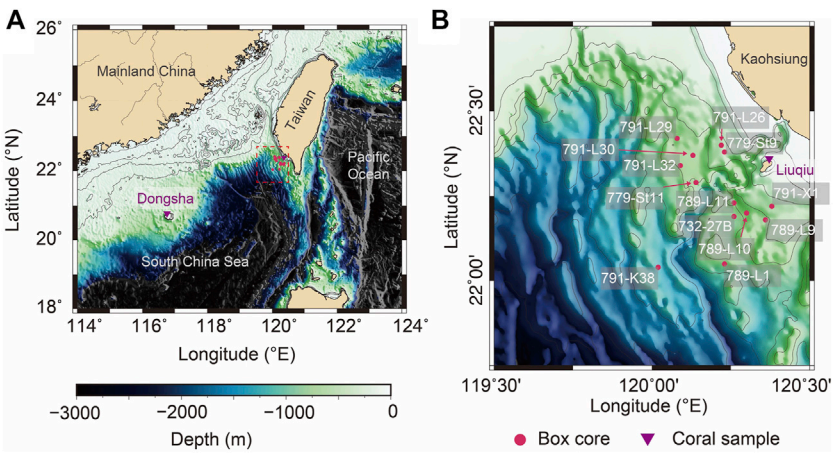

FIGURE 1 | (A) The location of Taiwan and Dongsha in the Western Pacific. Red circles represent the sampling locations of the box core, and purple triangles represent the sampling locations of the coral core. **(B)** is the enlarged segment of **(A)** marked with the red dash square and shows the location and label of the collected box cores.

Samples used for the radionuclide isotope analysis were sliced into sections with 2-cm intervals from the top of the sediment core. Each section was sealed in a plastic bag and stored in the refrigerator at 4°C before being freeze dried. After the sample was dried, the water content in the sediment sample was determined. Dried samples were then transferred to plastic jars (inside diameter is 8.5 cm; height is 7.5 cm) for nondestructive gamma spectrometric assay of radionuclides. Analyzed radionuclides include ^{210}Pb, ^{214}Pb, and ^{137}Cs, which were used as sediment chronometers (Huh et al., 2009) and were calculated according to a salt-free dry weight. The digital gamma-ray spectrometer was connected to HPGe detectors for counting radionuclides simultaneously based on photon peaks centering at 46.52 (^{210}Pb), 351.99 (^{214}Pb), and 661.62 (^{137}Cs) keV, respectively. Afterward, the counting results were analyzed with GammaVision 32 software (Su and Huh, 2002; Huh et al., 2006; Huh et al., 2009).

^{214}Pb is the precursor of ^{210}Pb and used as the index of supported ^{210}Pb ($^{210}Pb_{sup}$). An excess of ^{210}Pb ($^{210}Pb_{ex}$) can be obtained by subtracting the ^{214}Pb active concentration from the recorded ^{210}Pb ($^{210}Pb_{ex} = {}^{210}Pb_{mea} - {}^{210}Pb_{sup}$; (Huh et al., 2006; Huh et al., 2009). ^{137}Cs could be measured simultaneously with ^{210}Pb by nondestructive gamma spectrometry, but it took a long time to obtain ^{137}Cs data due to the lower activity. Therefore, only

TABLE 2 | Linear regression analyses of $\delta^{13}C$ from 1900 to the present.

From 1900 to the present					
	Slope	**Intercept**	**r Squared**	***p*-Value**	**Number**
732-27B	–0.008	16.408	0.504	0.001	19
779-St9	–0.036	72.188	0.722	0.016	7
779-St11	–0.005	10.758	0.677	0.087	5
789-L1	–0.006	13.505	0.608	0.013	9
789-L9	–0.009	18.893	0.417	<0.001	44
789-L10	–0.004	10.022	0.348	0.005	21
789-L11	–0.008	16.261	0.525	<0.001	38
791-K38	–0.009	18.113	0.753	0.001	10
791-L26	–0.018	37.592	0.691	0.011	8
791-L29	–0.006	12.949	0.430	<0.001	38
791-L30	–0.007	14.502	0.401	<0.001	28
791-L32	–0.006	12.154	0.375	<0.001	31
791-X1	–0.009	19.375	0.582	<0.001	40
All samples ($p \leq 0.05$)	–0.008	16.125	0.445	0.000	293
Dongsha			Only after 1960		
Liuqiu	–0.015	26.622	0.386	<0.001	988

TABLE 3 | Linear regression analyses of $\delta^{13}C$ from 1960 to the present.

From 1960 to the present					
	Slope	**Intercept**	**r Squared**	***p*-Value**	**Number**
732-27B	–0.011	23.565	0.445	0.050	9
779-St9	–0.038	75.565	0.648	0.053	6
779-St11	–0.003	7.231	0.441	0.336	4
789-L1	–0.007	15.621	0.630	0.206	4
789-L9	–0.019	37.681	0.565	<0.001	24
789-L10	–0.007	14.883	0.263	0.088	12
789-L11	–0.016	33.490	0.538	0.001	18
791-K38	–0.010	20.469	0.396	0.255	5
791-L26	–0.019	38.339	0.496	0.077	7
791-L29	–0.020	40.522	0.683	<0.001	20
791-L30	–0.018	37.689	0.510	0.004	14
791-L32	–0.011	23.695	0.388	0.023	13
791-X1	–0.020	41.079	0.732	<0.001	24
All samples ($p \leq 0.05$)	–0.016	32.492	0.493	<0.001	122
Dongsha	–0.031	59.676	0.314	<0.001	289
Liuqiu	–0.022	41.844	0.410	<0.001	623

a portion of the cores were analyzed for ^{137}Cs to constrain the ^{210}Pb chronology. More details of the gamma spectrometry analysis are described in Huh et al. (2009).

Sedimentation rates derived from fallout radionuclides (^{210}Pb and ^{137}Cs) indicate constant hemipelagic accumulation, which implies that collected cores are suitable for reconstructing the recent paleoenvironment (Huh et al., 2009). The two out of 92 sediment cores (789-L1 and 791-K38) were selected as representatives in our study because of ample planktonic and benthic foraminiferal shells and the well age dating of box cores.

Ages of core samples at different depths were estimated by the sedimentation rate of each core. The linear regression of each core between $\delta^{13}C$ values of foraminifera shells and ages of samples was performed by the least square method using FITLM function provided by MATLAB R2020 software (Street et al., 1988). The two datasets, age later than 1900s and later than 1960s, were screened for regression analyses to compare with published records. Results of regression are listed in **Tables 2** and **3** (e.g., slope, intercept, r squared, *p* value, and number of samples).

Coral skeletal records from Dongsha (Ren et al., 2017) and Liuqiu were also included to compare the anthropogenic effects on the two reef sites (**Figure 1**). The coral skeletal core collected around Liuqiu (120.36°E, 22.35°N) was drilled from a living *Porites* sp. colony at a depth of about 10 m on June 29, 2017. The core was cut into two slabs, then scanned by x-rays to identify its maximum growth axis, and then subsampled with an automated three-axis saw machine. Skeletal pieces (11 mm × 1 mm × 2.5 mm) with about monthly resolution were cut along the maximum growth axis and crushed into powder. About 5% of the powder is used for $\delta^{13}C$ and $\delta^{18}O$ analyses with isotope ratio mass spectrometer in the Stable Isotope Laboratory at the Department of Earth Science in National Normal University.

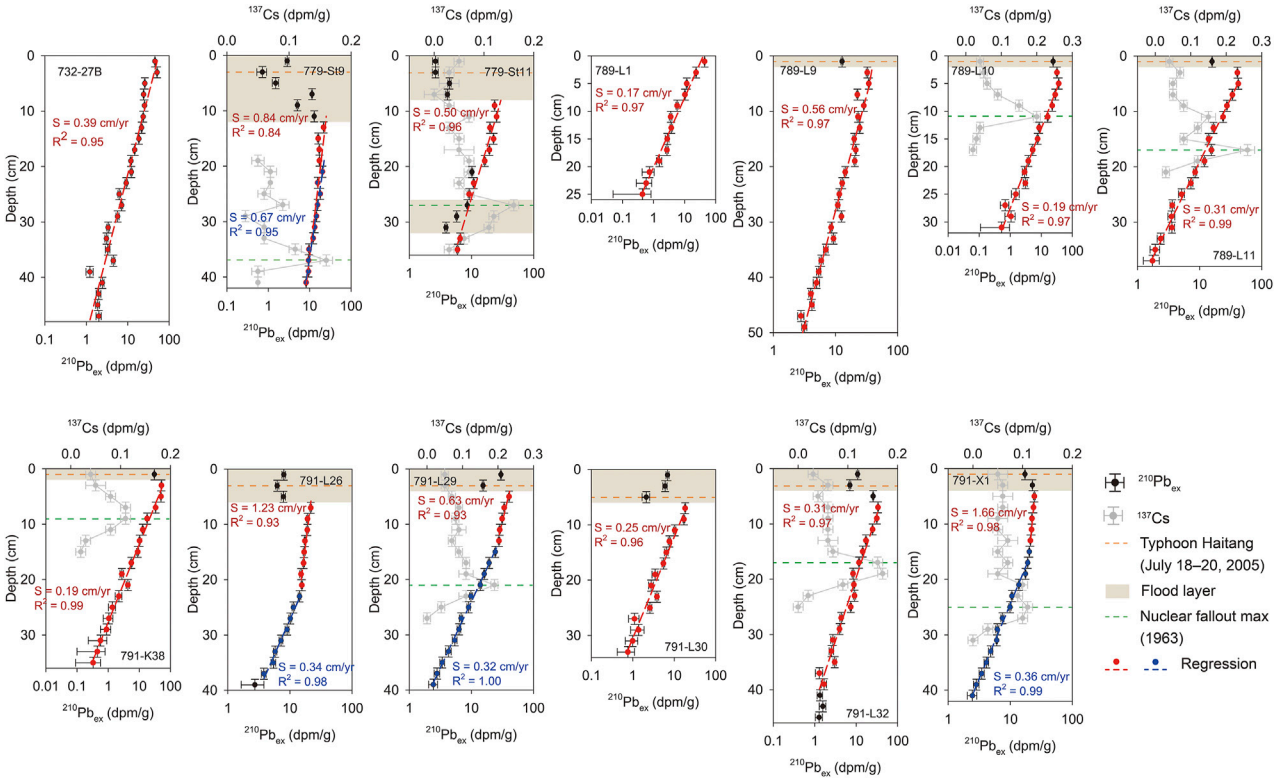

FIGURE 2 | The $^{210}Pb_{ex}$ profile in each sediment core (black dots) shows a good fit ($R^2 > 0.93$) with a steady-state advection-decay model. The red and blue dots represent the selected fitting points, and the dashed line of each color represents the corresponding fitting results. The black dots that are not marked by color are not included in the fit, usually in the flood event layer. The ^{137}Cs profile is represented by gray dots. The control points in the age model, the maximum value of ^{137}Cs and Typhoon Haitang, are represented by green and orange dashed lines, respectively [The data of $^{210}Pb_{ex}$ and ^{137}Cs was from Huh et al., (2009)]. Brown patches in the core top indicate the event layer (flood layer).

The remaining powder is saved for other analysis. Combined with annual growth bands in x-ray images, skeletal $\delta^{18}O$ was compared with the extended reconstructed sea surface temperature (ERSSTv5) of the NOAA to establish the age model.

RESULTS AND DISCUSSION

The chronology of sediment cores

In general, ^{210}Pb in marine sediments is influenced by two factors: 1) the decay of ^{226}Ra of marine sediments, $^{210}Pb_{sup}$, and 2) the decay of atmospheric ^{222}Rn, which deposits into the ocean and is preserved in marine sediments by the removal of particles from the water column, expressed as $^{210}Pb_{ex}$ (Hung and Chung, 1998). The depletion of $^{210}Pb_{ex}$ causes the ^{210}Pb activity to decrease exponentially or quasi-exponentially along the downcore until total ^{210}Pb activity in the sediment is equal to $^{210}Pb_{sup}$. In short, the $^{210}Pb_{ex}$ profile represents the stable deposition if $^{210}Pb_{ex}$ decays exponentially with the depth and can be explained by the steady-state advection-decay model (Huh et al., 2009).

Assuming the amount of the sediment and ^{210}Pb flux at a given site are constant, and the mixing in the sediment is ignored. The downcore of $^{210}Pb_{ex}$ profile is, thus, invariable with time and described by:

$$ln C_z = ln C_0 - \frac{\lambda}{S} Z \quad (1)$$

where C_0 and C_z are $^{210}Pb_{ex}$ at the sediment–water interface and depth Z, respectively. λ is the decay constant (0.0311 year^{-1}) of ^{210}Pb, and S is the sedimentation rate (cm year^{-1}). Based on the regression analysis of $^{210}Pb_{ex}$ (**Eq. 1**), the linear sedimentation rate can be calculated (Holmes, 1998; Lewis et al., 2002; Huh et al., 2009).

Most of the $^{210}Pb_{ex}$ in the collected sediment cores decreased exponentially downcore with a few layers having low $^{210}Pb_{ex}$ values (**Figure 2**). The characteristics of $^{210}Pb_{ex}$ profiles were separated into Type I (sediment deposition in nonreworked settings; e.g., 789-L1), Type III (the existence of a physically and/or biological reworked surficial layer; e.g., 779-St11), and Type V (influenced by strong episodic events; e.g., 779-St9) according to the classification described by Xu et al. (2015). After excluding bio-interferences and event layers, the sedimentation rate and the preliminary age model of the 13 sediment cores were estimated.

^{137}Cs was introduced as the control point of the $^{210}Pb_{ex}$-derived age model in collected sediment cores. The ^{137}Cs profile had the typical maximum radioisotope activity in the subsurface (the anthropogenic nuclide in 1963 A.D.) in which

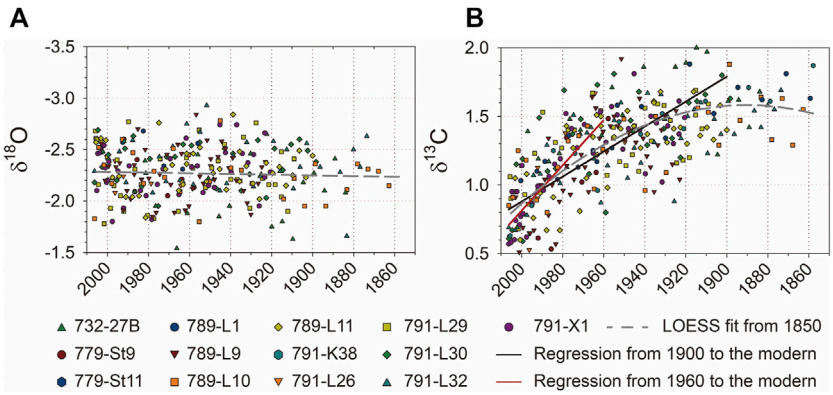

FIGURE 3 | δ^{18}O and δ^{13}C derived from planktonic foraminifera *G. sacculifer* of 13 box cores are shown in **(A)** and **(B)**, respectively. LOESS fit from 1850 to the present was plotted as the gray line. Linear regressions of δ^{13}C from 1900 to the present and from 1960 to the present were plotted as blue and red lines, respectively. Different symbols with colors indicate box cores collected near Liuqiu.

^{137}Cs decreased gradually upward but sharply downward (Holmes, 1998; Huh et al., 2009; **Figure 2**). Since the ^{210}Pb-derived age model matches the control point indicated by ^{137}Cs, the quality of ^{210}Pb dating is reliable.

Additionally, the interference by the typhoon was considered as another control point of the age model in our study. For example, the intense rainfall caused flood deposits in the downstream shelf during Super Typhoon Haitang occurring on July 18–20, 2005 (Huh et al., 2009). This resulted in a low $^{210}Pb_{ex}$ layer occupying on the sediment core top collected afterward, especially for cores obtained in the same year of the typhoon event (e.g., 779-St9 and 779-St11 in **Figure 2**). The $^{210}Pb_{ex}$ profile implies the typhoon event did not interfere with the ^{210}Pb-derived age model severely in the long-term scale because the event layer (indicated by the minimum $^{210}Pb_{ex}$ value) was gradually buried by accumulating pelagic or hemipelagic sediments. Eventually, the event signal with low $^{210}Pb_{ex}$ was diluted and became weaker, though the signal was still observed in some of the collected sediment cores.

Isotopes in planktonic Foraminifera

Oxygen and carbon isotopes of *G. sacculifer* in 13 box cores were plotted in **Figure 3**. Of the δ^{18}O data, 84% ranged between −2.5‰ and −2‰ for the last 150 years from 2010 (**Figure 3A**). The δ^{13}C records, however, fluctuated around 1.5‰ and started to decline after the 1900s followed by the rapid decline trend after the 1960s (**Figure 3B**). Both oxygen and carbon isotopic compositions from coretops were consistent with modern shells collected by sediment traps in this regime (Lin, 2014). To decipher historical isotopic changes, two out of 13 cores, 789-L1 and 791-K38, were selected as the representatives. The isotopes generated from planktonic foraminifera *G. sacculifer* and benthic foraminifera *Uvigerina sp.* are shown in **Figures 4A–D**. The planktonic isotopes of the other 11 cores are shown in **Supplementary Figure S1**.

The δ^{18}O variability in core samples

The range and fluctuation pattern of planktonic δ^{18}O of two selected downcore records were very similar, particularly the broad δ^{18}O-enriched interval between 1950 and 1990 (**Figure 4A**). The deceasing of δ^{18}O occurring between 1950 and 1970 followed by a rising trend until 1990 was also observed in local meteorological data (Shiu et al., 2009). However, the planktonic δ^{18}O was consistent overall.

Unlike the relatively continuous planktonic record, the benthic δ^{18}O for core 789-L1 was discrete due to insufficient foraminiferal shells at specific layers of the sediment core (**Figure 4B**). Despite the limited number of measured shells, δ^{18}O values of *Uvigerina* sp. from core 789-L1 were generally lighter than that of core 791-K38. Mulitza et al. (2003) has described that the increase in δ^{18}O is induced by the temperature drop, regardless of salinity effect. Therefore, the offset in benthic δ^{18}O records (2.2‰ for 789-L1 vs. 2.9‰ for 791-K38 in average between 1910–1940) could be attributed to the different water temperatures between two coring sites (5.51°C at 911 m for 789-L1 vs. 3.45°C at 1,260 m for 791-K38 according to the hydrographic data). However, the variability of the regional upwelling should be another potential factor to change benthic δ^{18}O (Wang et al., 2008).

Generally speaking, the planktonic δ^{18}O corresponded well with the change in the local surface temperature, and benthic δ^{18}O values were controlled by the temperature gradient at the sampled water depth or the regional ocean circulation. There is no further evidence indicating that human activities influenced δ^{18}O values in marine sediments in the nearshore realm.

The δ^{13}C trend in core samples and anthropogenic carbon effects

The carbon isotope composition of *G. sacculifer* of two selected cores are shown in **Figure 4C**. Unlike the coherent pattern in planktonic δ^{18}O records (**Figure 4A**), the time-series of planktonic δ^{13}C showed a 1‰–1.5‰ decline trend for the last

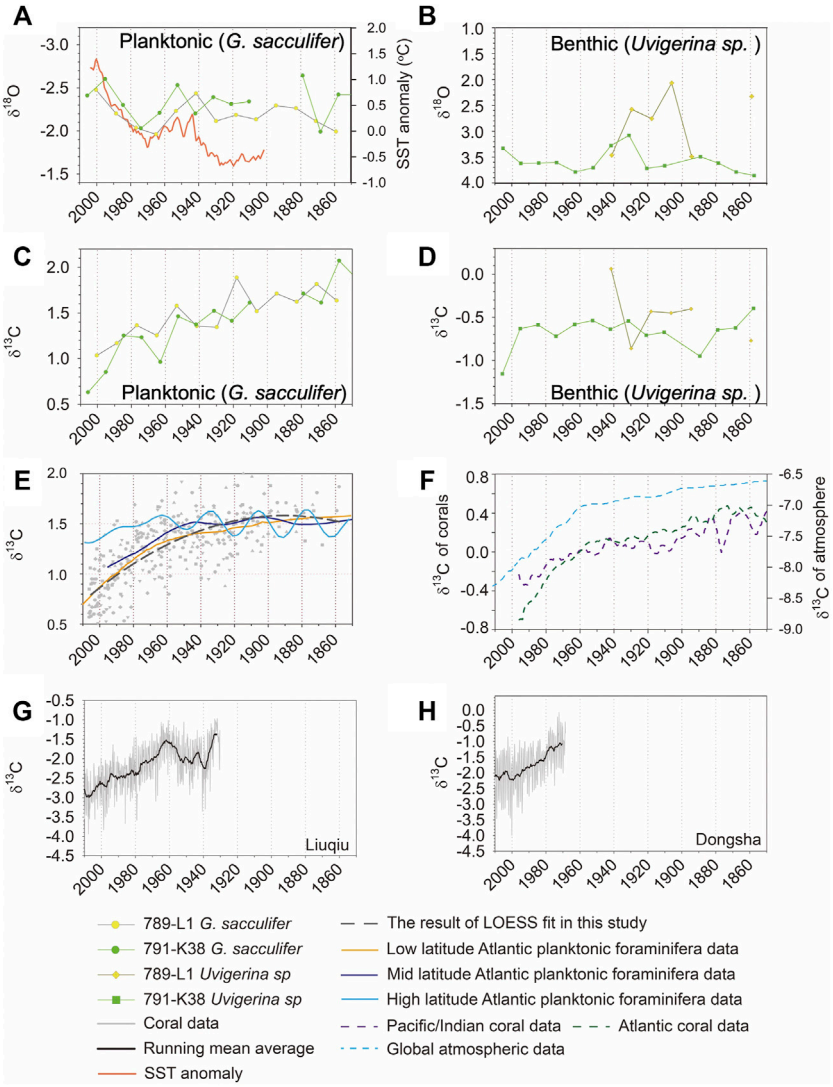

FIGURE 4 | (A) The $\delta^{18}O$ of *G. sacculifer* in core 789-L1 and 791-K38 combine with the anomaly of sea surface temperature around Taiwan (adopted from Shiu et al., 2009). **(B)** The $\delta^{18}O$ of *Uvigerina* sp. in core 789-L1 and 791-K38. **(C)** The $\delta^{13}C$ of *G. sacculifer* in core 789-L1 and 791-K38. **(D)** The $\delta^{13}C$ of *Uvigerina* sp. in core 789-L1 and 791-K38. **(E)** The light gray symbol shows all the $\delta^{13}C$ of planktonic foraminifers in this study, and the LOESS fit represent the situation in the mid-low latitude Pacific Ocean. The orange, purple, and light blue lines represent the situation of planktonic foraminifera in the Atlantic Ocean at low, mid, and high latitudes, respectively (adopted from Black et al., 2011; Mellon et al., 2019; Simon et al., 2020). The $\delta^{13}C$ axis of these three data sets was shifted to facilitate comparison with our data. **(F)** The $\delta^{13}C$ of corals in the Atlantic and the Pacific/Indian Oceans (green and purple lines; adopted from Swart et al., 2010), and the global $\delta^{13}C$ of atmosphere (light blue line; Graven et al., 2017). **(G)** The $\delta^{13}C$ of coral record from Liuqiu. **(H)** The $\delta^{13}C$ of coral record from Dongsha. The gray line represents the raw data, and the black line is the 4-year running mean average.

century. Particularly, the decline trend since 1960 is a pervasive feature showing in all collected sediment cores (**Figure 3B**), which also followed the depletion trend of $\delta^{13}C$ in the atmospheric CO_2 (**Figure 4H**). Since the planktonic $\delta^{18}O$ did not present a corresponding decline (or incline) trend during the same period (**Figures 3A** and **4A**), the depletion of the planktonic $\delta^{13}C$ was not attributed to the temperature change (Goericke and Fry, 1994; Dixit et al., 2015). The results highlight the creditability of foraminiferal records for identifying the ^{13}C Suess effect in the nearshore off southwestern Taiwan.

The decline trend of $\delta^{13}C$ in the surface ocean was caused by the input of radiocarbon-dead or anthropogenic-produced ^{13}C-depleted carbons from the atmosphere through the air–sea exchange process (Suess, 1955; Keeling, 1979; Broecker and Maier-Reimer, 1992; Quay et al., 1992). The ^{13}C-depleted carbon has been widely reported in coral skeleton and sclerosponge (Druffel and Benavides, 1986; Swart et al., 1996a; Swart et al., 1996b; Swart et al., 2010; Al-Rousan and Felis, 2013; Hou et al., 2019; Liu et al., 2021) and planktonic foraminifera (Al-Rousan et al., 2004; Black et al., 2011; Xu et al., 2014; Mellon et al.,

2019; Simon et al., 2020), while the downcore variability of the benthic $\delta^{13}C$ was rather flat and restricted within 0.51‰–1‰ in our study area (**Figure 4D**). This implies that the penetration of the anthropogenic carbon only occurred in the upper water column at our study site. Although other processes could influence the $\delta^{13}C$ of benthic foraminifera (Mccorkle et al., 1990; Schmittner et al., 2017), our results were consistent as the previous finding by Sabine et al. (2004).

The similar magnitude of planktonic $\delta^{13}C$ decline from the 1900s were around 0.6‰ and 0.9‰ for cores 789-L1 and 791-K38, respectively (the decline rate for each core was shown as the slope in **Table 2**). The similar range in the decline of $\delta^{13}C$ was first noted by corals and sclerosponges with 0.5‰ between 1850 and 1975 from Bermuda (Nozaki et al., 1978) and Jamaica (Druffel and Benavides, 1986). The global average rate of change in the coral skeletal $\delta^{13}C$ was estimated as −0.01‰ year^{-1} from 1900 to 1990 based on a compilation of coral records throughout the oceans (Swart et al., 2010). However, the decline rates of $\delta^{13}C$ in the Indian, Pacific, and Atlantic Oceans were different during 1960–1990. The rate in the Atlantic Ocean was −0.019‰ year^{-1}, but in the Pacific and the Indian Ocean, it was around −0.007‰ year^{-1} (Swart et al., 2010). The differences could be caused by physiological activities of corals or bathymetric conditions, which change the $\delta^{13}C_{DIC}$ [dissolved inorganic carbon (DIC)] in the ambient seawater (Swart et al., 2010; Watanabe et al., 2017; Fujii et al., 2020; Simon et al., 2020).

To compare with previous coral records (Swart et al., 2010), the $\delta^{13}C$ used in this study was analyzed by the linear regression at two corresponding periods (1900 to the present and 1960 to the present, **Tables 2** and **3**). More than half of the sediment cores used in this study show the statistical significance in the depletion of $\delta^{13}C$ ($p < 0.05$) toward the present (**Table 2**). From 1900 to the present, the average decline rate of the $\delta^{13}C$ in planktonic foraminiferal records was about 0.008‰ year^{-1}, which was similar to the findings of the global coral. From 1960 to the present, the average decline rate of the $\delta^{13}C$ significantly increased to 0.016‰ year^{-1}, which was higher than published coral records in the Pacific Ocean but was close to the value of coral measurements in the Atlantic Ocean (Swart et al., 2010). Although the decline rate was different from the previous record in the Pacific Ocean, our findings suggest that the $\delta^{13}C$ Suess effect at the surface water of the Pacific Ocean might be as strong as that of the Atlantic Ocean, which is consistent with the global estimation by Eide et al. (2017).

Although there were isotopic offsets between precipitated calcium carbonate shells and the ambient seawater, Mellon et al. (2019) have indicated that decline trends of the $\delta^{13}C$ recorded by different species of foraminiferal were still consistent. To compare $\delta^{13}C$ among different planktonic foraminiferal records, data published in previous studies were digitalized and plotted with the long-term variability of measured planktonic $\delta^{13}C$ in this study (**Figure 4E**). Our measurement was depicted by LOESS fit (Mellon et al., 2019) and showed a similar trend to planktonic foraminiferal records in the lower latitudes of the Atlantic, both in terms of the overall decline magnitude in, and the enhanced decline rate after, the 1960s. However, there were differences in the $\delta^{13}C$ trend found in the higher latitudes of the Atlantic. Our planktonic records showed a larger decreasing range of $\delta^{13}C$ than that found in mid to high latitude of the Atlantic, though the rapid decline trend also occurred after the 1960s. The differences have been described by Eide et al. (2017) indicating that the ^{13}C Suess effect in the surface seawater is relatively uniform in the North Pacific and North Atlantic but slightly lower in the mid-high latitudes. In the Atlantic, the decline range of $\delta^{13}C$ in foraminiferal records was less than 0.3‰ (−0.007‰ year^{-1}) in high latitude, about 0.4‰ (−0.010‰ year^{-1}) in the middle latitude, and close to 0.7‰ (−0.018‰ year^{-1}) in the low latitude (Black et al., 2011; Mellon et al., 2019; Simon et al., 2020). The lower ^{13}C Suess effect occurring in the higher latitudes of the Atlantic was attributed to local ocean circulations and primary productivities (Mellon et al., 2019; Simon et al., 2020).

The collected foraminiferal and coral records in sediment cores were further compared with the coral records obtained at Liuqiu (high human impact and close to the coring sites of foraminiferal records) and Dongsha (less human impact). The $\delta^{13}C$ trends in foraminiferal and coral records were consistent, and its decline rates were similar (**Figures 4C, F–H**). The slopes of the Liuqiu and Dongsha coral records after the 1960s were −0.022 and −0.031‰ year^{-1}, respectively (**Table 3**), which were also higher than that in the published records of Pacific corals. Obviously, the similar $\delta^{13}C$ trend found in foraminiferal and coral records was not influenced by the local effect since the distance between Liuqiu and Dongsha is 412 km away (**Figure 1**), so global ^{13}C Suess effect is considered to explain the extensive effect on the records of these two regions. This indicates that planktonic records of sediment cores collected off southwestern Taiwan are suitable to represent the anthropogenic signal of $\delta^{13}C$ in the last century.

CONCLUSION

Our results show that the $\delta^{13}C$ of planktonic foraminifera off southwestern Taiwan in the Western Pacific has decreased by 1‰–1.5‰ over the last century. From the 1900 to the present, the decline trend was about 0.008‰ year^{-1}, which became steeper to 0.016‰ year^{-1} after the 1960s. The decline trend of $\delta^{13}C$ found in our foraminiferal samples was higher than that in previous coral records in the Pacific and consistent with that in the Atlantic coral records, which presented a similar decline trend in global atmospheric CO_2. The decreasing $\delta^{13}C$ in planktonic foraminiferal records was attributed to the additional anthropogenic CO_2 input, which is regarded as the Suess effect. Such anthropogenic carbon signal was only observed in the upper water column according to the planktonic and benthic foraminiferal records. Since the variability of $\delta^{13}C$ in foraminiferal records were highly consistent with that in coral records collected at Liuqiu and Dongsha, the SCS, our findings suggest that carbon isotopes on a centennial scale could be reconstructed in the nearshore region with well age-controlled sediment cores. Therefore, the nearshore sediment core potentially complements the lack of $\delta^{13}C$ records in specific areas where coral growth is restricted.

DATA AVAILABILITY STATEMENT

The original contributions presented in the study are included in the article/**Supplementary Material**. Further inquiries can be directed to the corresponding author.

AUTHOR CONTRIBUTIONS

JL and RY performed the simulation and prepared the manuscript. HL conceived and designed the study, handled the sedimentary records, and co-wrote the manuscript. YC and R-YC-L handled the coral records in Liuqiu and Dongsha. HR contributed to the interpretation of the coral records. JTL is the leader of the FATES Program and supervised the work.

FUNDING

This study was funded by the Ministry of Science and Technology grants (Nos. NSC 96-2611-M-110-009 and MOST 108-2611- M-110-012).

ACKNOWLEDGMENTS

We are grateful to Dr. Salwood Lin at the Institute of Oceanography, National Taiwan University, for collecting the sediment cores applied in this research. Bo-Shian Wang, Tsai-Luen Yu, and Chiuan-Sheng Liu sampled the Liuqui (Xiaoliuqiu) coral core. Prof. Hong-Chun Li at the Department of Geosciences, National Taiwan University, and Prof. Horng-Sheng Mii at the Department of Earth Sciences, National Taiwan Normal University, are acknowledged for their help with the stable isotope analyses. Our sincere gratitude to Tai-Chun Lin for her assistance in the laboratory.

SUPPLEMENTARY MATERIAL

The Supplementary Material for this article can be found online at: https://www.frontiersin.org/articles/10.3389/feart.2021.795519/full#supplementary-material

REFERENCES

Al-Rousan, S., and Felis, T. (2013). Long-term Variability in the Stable Carbon Isotopic Composition of Porites Corals at the Northern Gulf of Aqaba, Red Sea. *Palaeogeogr. Palaeoclimatol. Palaeoecol.* 381-382, 1–14. doi:10.1016/j.palaeo.2013.03.025

Al-Rousan, S., Patzold, J. r., Al-Moghrabi, S., and Wefer, G. (2004). Invasion of Anthropogenic CO2 Recorded in Planktonic Foraminifera from the Northern Gulf of Aqaba. *Int. J. Earth Sci. (Geol Rundsch)* 93, 1066–1076. doi:10.1007/s00531-004-0433-4

Archer, D., Kheshgi, H., and Maier-Reimer, E. (1998). Dynamics of Fossil Fuel CO2neutralization by marine CaCO3. *Glob. Biogeochem. Cycles* 12, 259–276. doi:10.1029/98gb00744

Black, D. E., Abahazi, M. A., Thunell, R. C., Kaplan, A., Tappa, E. J., and Peterson, L. C. (2007). An 8-century Tropical Atlantic SST Record from the Cariaco Basin: Baseline Variability, Twentieth-century Warming, and Atlantic hurricane Frequency. *Paleoceanography* 22, PA4204. doi:10.1029/2007pa001427

Black, D., Thunell, R., Wejnert, K., and Astor, Y. (2011). Carbon Isotope Composition of Caribbean Sea Surface Waters: Response to the Uptake of Anthropogenic CO2. *Geophys. Res. Lett.* 38, L16609. doi:10.1029/2011gl048538

Broecker, W. S., and Maier-Reimer, E. (1992). The Influence of Air and Sea Exchange on the Carbon Isotope Distribution in the Sea. *Glob. Biogeochem. Cycles* 6, 315–320. doi:10.1029/92gb01672

Crutzen, P. J., and Stoermer, E. F. (2000). The "Anthropocene". *Glob. Change Newsl.* 41, 17. .

Damon, P. E., Lerman, J. C., and Long, A. (1978). Temporal Fluctuations of Atmospheric 14C: Causal Factors and Implications. *Annu. Rev. Earth Planet. Sci.* 6, 457–494. doi:10.1146/annurev.ea.06.050178.002325

Dixit, Y., Hodell, D. A., Sinha, R., and Petrie, C. A. (2015). Oxygen Isotope Analysis of Multiple, Single Ostracod Valves as a Proxy for Combined Variability in Seasonal Temperature and lake Water Oxygen Isotopes. *J. Paleolimnol* 53, 35–45. doi:10.1007/s10933-014-9805-3

Druffel, E. R. M., and Benavides, L. M. (1986). Input of Excess CO2 to the Surface Ocean Based on 13C/12C Ratios in a Banded Jamaican Sclerosponge. *Nature* 321, 58–61. doi:10.1038/321058a0

Eide, M., Olsen, A., Ninnemann, U. S., and Eldevik, T. (2017). A Global Estimate of the Full Oceanic 13 C Suess Effect since the Preindustrial. *Glob. Biogeochem. Cycles* 31, 492–514. doi:10.1002/2016GB005472

Farquhar, G. D., Ehleringer, J. R., and Hubick, K. T. (1989). Carbon Isotope Discrimination and Photosynthesis. *Annu. Rev. Plant Physiol. Plant Mol. Biol.* 40, 503–537. doi:10.1146/annurev.pp.40.060189.002443

Field, C. B., and Raupach, M. R. (2004). *The Global Carbon Cycle: Integrating Humans, Climate, and the Natural World*. Washington DC: Island Press.

Friedli, H., Lötscher, H., Oeschger, H., Siegenthaler, U., and Stauffer, B. (1986). Ice Core Record of the 13C/12C Ratio of Atmospheric CO2 in the Past Two Centuries. *Nature* 324, 237–238. doi:10.1038/324237a0

Fujii, T., Tanaka, Y., Maki, K., Saotome, N., Morimoto, N., Watanabe, A., et al. (2020). Organic Carbon and Nitrogen Isoscapes of Reef Corals and Algal Symbionts: Relative Influences of Environmental Gradients and Heterotrophy. *Microorganisms* 8, 1221. doi:10.3390/microorganisms8081221

Gaskell, D. E., and Hull, P. M. (2019). Symbiont Arrangement and Metabolism Can Explain High δ13C in Eocene Planktonic Foraminifera. *Geology* 47, 1156–1160. doi:10.1130/g46304.1

Goericke, R., and Fry, B. (1994). Variations of marine Plankton δ13C with Latitude, Temperature, and Dissolved CO2in the World Ocean. *Glob. Biogeochem. Cycles* 8, 85–90. doi:10.1029/93gb03272

Graven, H., Keeling, R. F., and Rogelj, J. (2020). Changes to Carbon Isotopes in Atmospheric CO 2 over the Industrial Era and into the Future. *Glob. Biogeochem. Cycles* 34, e2019GB006170. doi:10.1029/2019gb006170

Graven, H., Allison, C.-E., and Etheridge, D. M. (2017). Compiled Records of Carbon Isotopes in Atmospheric CO*2* for Historical Simulations in CMIP6. *Geosci. Model. Dev.* 10(12), 4405–4417. doi:10.5194/gmd-10-4405-2017

Grottoli, A. G., and Wellington, G. M. (1999). Effect of Light and Zooplankton on Skeletal δ 13 C Values in the Eastern Pacific Corals Pavona Clavus and Pavona Gigantea. *Coral Reefs* 18, 29–41. doi:10.1007/s003380050150

Hansen, G., and Stone, D. (2016). Assessing the Observed Impact of Anthropogenic Climate Change. *Nat. Clim Change* 6, 532–537. doi:10.1038/nclimate2896

Holmes, C. W. (1998). "Short-lived Isotopic Chronometers: a Means of Measuring Decadal Sedimentary Dynamics," in *Fact Sheet*. U.S. Geological Survey. doi:10.3133/fs07398

Höök, M., and Tang, X. (2013). Depletion of Fossil Fuels and Anthropogenic Climate Change-A Review. *Energy Policy* 52, 797–809. doi:10.1016/j.enpol.2012.10.046

Hou, A., Halfar, J., Adey, W., Wortmann, U. G., Zajacz, Z., Tsay, A., et al. (2019). Long-lived Coralline Alga Records Multidecadal Variability in Labrador Sea Carbon Isotopes. *Chem. Geology.* 526, 93–100. doi:10.1016/j.chemgeo.2018.02.026

Huh, C.-A., Lin, H.-L., Lin, S., and Huang, Y.-W. (2009). Modern Accumulation Rates and a Budget of Sediment off the Gaoping (Kaoping) River, SW Taiwan: A Tidal and Flood Dominated Depositional Environment Around a Submarine canyon. *J. Mar. Syst.* 76, 405–416. doi:10.1016/j.jmarsys.2007.07.009

Huh, C.-A., Su, C.-C., Wang, C.-H., Lee, S.-Y., and Lin, I.-T. (2006). Sedimentation in the Southern Okinawa Trough - Rates, Turbidites and a Sediment Budget. *Mar. Geology.* 231, 129–139. doi:10.1016/j.margeo.2006.05.009

Hung, G. W., and Chung, Y.-C. (1998). Particulate Fluxes, 210Pb and 210Po Measured from Sediment Trap Samples in a canyon off Northeastern Taiwan. *Continental Shelf Res.* 18, 1475–1491. doi:10.1016/s0278-4343(98)00032-6

Jonkers, L., Van Heuven, S., Zahn, R., and Peeters, F. J. C. (2013). Seasonal Patterns of Shell Flux, δ18O and δ13C of Small and largeN.Pachyderma(s) andG.Bulloidesin the Subpolar North Atlantic. *Paleoceanography* 28, 164–174. doi:10.1002/palo.20018

Katz, M. E., Cramer, B. S., Franzese, A., Honisch, B., Miller, K. G., Rosenthal, Y., et al. (2010). Traditional and Emerging Geochemical Proxies in Foraminifera. *J. Foraminiferal Res.* 40, 165–192. doi:10.2113/gsjfr.40.2.165

Keeling, C. D. (1979). The Suess Effect: 13Carbon-14Carbon Interrelations. *Environ. Int.* 2, 229–300. doi:10.1016/0160-4120(79)90005-9

Kennedy, J. A., and Brassell, S. C. (1992). Molecular Records of Twentieth-century El Niño Events in Laminated Sediments from the Santa Barbara basin. *Nature* 357, 62–64. doi:10.1038/357062a0

Khatiwala, S., Primeau, F., and Hall, T. (2009). Reconstruction of the History of Anthropogenic CO2 Concentrations in the Ocean. *Nature* 462, 346–349. doi:10.1038/nature08526

Lewis, R. C., Coale, K. H., Edwards, B. D., Marot, M., Douglas, J. N., and Burton, E. J. (2002). Accumulation Rate and Mixing of Shelf Sediments in the Monterey Bay National Marine Sanctuary. *Mar. Geology.* 181, 157–169. doi:10.1016/S0025-3227(01)00265-1

Lin, H.-L. (2014). The Seasonal Succession of Modern Planktonic Foraminifera: Sediment Traps Observations from Southwest Taiwan Waters. *Continental Shelf Res.* 84, 13–22. doi:10.1016/j.csr.2014.04.020

Linsley, B. K., Dunbar, R. B., Dassié, E. P., Tangri, N., Wu, H. C., Brenner, L. D., et al. (2019). Coral Carbon Isotope Sensitivity to Growth Rate and Water Depth with Paleo-Sea Level Implications. *Nat. Commun.* 10, 2056. doi:10.1038/s41467-019-10054-x

Liu, J. T., Huh, C.-A., and You, C.-F. (2009). Fate of Terrestrial Substances in the Gaoping (Kaoping) Shelf/Slope and in the Gaoping Submarine Canyon off SW Taiwan. *J. Mar. Syst.* 76, 367–368. doi:10.1016/j.jmarsys.2008.08.005

Liu, X., Deng, W., Cui, H., Chen, X., Cai, G., Zeng, T., et al. (2021). Change of Coral Carbon Isotopic Response to Anthropogenic Suess Effect since Around 2000s. *Mar. Environ. Res.* 168, 105328. doi:10.1016/j.marenvres.2021.105328

Mcconnaughey, T. (1989). 13C and 18O Isotopic Disequilibrium in Biological Carbonates: I. Patterns. *Geochimica et Cosmochimica Acta* 53, 151–162. doi:10.1016/0016-7037(89)90282-2

Mccorkle, D. C., Keigwin, L. D., Corliss, B. H., and Emerson, S. R. (1990). The Influence of Microhabitats on the Carbon Isotopic Composition of Deep-Sea Benthic Foraminifera. *Paleoceanography* 5, 161–185. doi:10.1029/PA005i002p00161

Mellon, S., Kienast, M., Algar, C., Menocal, P., Kienast, S. S., Marchitto, T. M., et al. (2019). Foraminifera Trace Anthropogenic CO 2 in the NW Atlantic by 1950. *Geophys. Res. Lett.* 46, 14683–14691. doi:10.1029/2019gl084965

Mulitza, S., Boltovskoy, D., Donner, B., Meggers, H., Paul, A., and Wefer, G. (2003). Temperature: δ18O Relationships of Planktonic Foraminifera Collected from Surface Waters. *Palaeogeogr. Palaeoclimatol. Palaeoecol.* 202(1), 143–152. doi:10.1016/S0031-0182(03)00633-3

Nozaki, Y., Rye, D. M., Turekian, K. K., and Dodge, R. E. (1978). A 200 Year Record of Carbon-13 and Carbon-14 Variations in a Bermuda Coral. *Geophys. Res. Lett.* 5, 825–828. doi:10.1029/GL005i010p00825

Qiu, X., Li, T., Chang, F., Nan, Q., Xiong, Z., and Sun, H. (2014). Sea Surface Temperature and Salinity Reconstruction Based on Stable Isotopes and Mg/Ca of Planktonic Foraminifera in the Western Pacific Warm Pool during the Last 155 Ka. *Chin. J. Ocean. Limnol.* 32, 187–200. doi:10.1007/s00343-014-3073-y

Quay, P. D., Tilbrook, B., and Wong, C. S. (1992). Oceanic Uptake of Fossil Fuel CO 2 : Carbon-13 Evidence. *Science* 256, 74–79. doi:10.1126/science.256.5053.74

Raven, J. A., and Falkowski, P. G. (1999). Oceanic Sinks for Atmospheric CO2. *Plant Cel Environ* 22, 741–755. doi:10.1046/j.1365-3040.1999.00419.x

Raza, T., Ahmad, S. M., Steinke, S., Raza, W., Lone, M. A., Beja, S. K., et al. (2017). Glacial to Holocene Changes in Sea Surface Temperature and Seawater δ18O in the Northern Indian Ocean. *Palaeogeogr. Palaeoclimatol. Palaeoecol.* 485, 697–705. doi:10.1016/j.palaeo.2017.07.026

Regnier, P., Friedlingstein, P., Ciais, P., Mackenzie, F. T., Gruber, N., Janssens, I. A., et al. (2013). Anthropogenic Perturbation of the Carbon Fluxes from Land to Ocean. *Nat. Geosci* 6, 597–607. doi:10.1038/ngeo1830

Ren, H., Chen, Y.-C., Wang, X. T., Wong, G. T. F., Cohen, A. L., Decarlo, T. M., et al. (2017). 21st-century Rise in Anthropogenic Nitrogen Deposition on a Remote Coral Reef. *Science* 356, 749–752. doi:10.1126/science.aal3869

Sabine, C. L., Feely, R. A., Gruber, N., Key, R. M., Lee, K., Bullister, J. L., et al. (2004). The Oceanic Sink for Anthropogenic CO 2. *Science* 305, 367–371. doi:10.1126/science.1097403

Schimmelmann, A., Lange, C. B., and Berger, W. H. (1990). Climatically Controlled Marker Layers in Santa Barbara Basin Sediments and fine-scale Core-To-Core Correlation. *Limnology and Oceanography* 35, 165–173.

Schmittner, A., Bostock, H. C., Cartapanis, O., Curry, W. B., Filipsson, H. L., Galbraith, E. D., et al. (2017). Calibration of the Carbon Isotope Composition (δ 13 C) of Benthic Foraminifera. *Paleoceanography* 32, 512–530. doi:10.1002/2016pa003072

Shackleton, N. (1967). Oxygen Isotope Analyses and Pleistocene Temperatures Re-assessed. *Nature* 215, 15–17. doi:10.1038/215015a0

Shiu, C.-J., Liu, S. C., and Chen, J.-P. (2009). Diurnally Asymmetric Trends of Temperature, Humidity, and Precipitation in Taiwan. *J. Clim.* 22, 5635–5649. doi:10.1175/2009jcli2514.1

Simon, M. H., Muschitiello, F., Tisserand, A. A., Olsen, A., Moros, M., Perner, K., et al. (2020). A Multi-Decadal Record of Oceanographic Changes of the Past ~165 Years (1850-2015 AD) from Northwest of Iceland. *PLOS ONE* 15, e0239373. doi:10.1371/journal.pone.0239373

Spero, H. J., and Williams, D. F. (1988). Extracting Environmental Information from Planktonic Foraminiferal δ13C Data. *Nature* 335, 717–719. doi:10.1038/335717a0

Street, J. O., Carroll, R. J., and Ruppert, D. (1988). A Note on Computing Robust Regression Estimates via Iteratively Reweighted Least Squares. *The Am. Statistician* 42, 152–154. doi:10.1080/00031305.1988.10475548

Su, C.-C., and Huh, C.-A. (2002). 210Pb, 137Cs and 239,240Pu in East China Sea Sediments: Sources, Pathways and Budgets of Sediments and Radionuclides. *Mar. Geology.* 183, 163–178. doi:10.1016/s0025-3227(02)00165-2

Suess, H. E. (1955). Radiocarbon Concentration in Modern Wood. *Science* 122, 415–417. doi:10.1126/science.122.3166.415.b

Swart, P. K., Dodge, R. E., and Hudson, H. J. (1996a). A 240-year Stable Oxygen and Carbon Isotopic Record in a Coral from South Florida: Implications for the Prediction of Precipitation in Southern Florida. *Palaios* 11, 362–375. doi:10.2307/3515246

Swart, P. K., Greer, L., Rosenheim, B. E., Moses, C. S., Waite, A. J., Winter, A., et al. (2010). The13C Suess Effect in Scleractinian Corals Mirror Changes in the Anthropogenic CO*2* inventory of the Surface Oceans. *Geophys. Res. Lett.* 37, L05604. doi:10.1029/2009gl041397

Swart, P. K., Healy, G. F., Dodge, R. E., Kramer, P., Hudson, J. H., Halley, R. B., et al. (1996b). The Stable Oxygen and Carbon Isotopic Record from a Coral Growing in Florida Bay: A 160 Year Record of Climatic and Anthropogenic Influence. *Palaeogeogr. Palaeoclimatol. Palaeoecol.* 123, 219–237. doi:10.1016/0031-0182(95)00078-x

Takahashi, T., Olafsson, J., Goddard, J. G., Chipman, D. W., and Sutherland, S. C. (1993). Seasonal Variation of CO2and Nutrients in the High-Latitude Surface Oceans: A Comparative Study. *Glob. Biogeochem. Cycles* 7, 843–878. doi:10.1029/93GB02263

Tao, K., Robbins, J. A., Grossman, E. L., and O'dea, A. (2013). Quantifying Upwelling and Freshening in Nearshore Tropical American Environments Using Stable Isotopes in Modern Gastropods. *Bms* 89, 815–835. doi:10.5343/bms.2012.1065

Thunell, R., Tappa, E., Pride, C., and Kincaid, E. (1999). Sea-surface Temperature Anomalies Associated with the 1997-1998 El Niño Recorded in the Oxygen Isotope Composition of Planktonic Foraminifera. *Geol* 27, 843–846. doi:10.1130/0091-7613(1999)027<0843:sstaaw>2.3.co;2

Wang, Y. H., Lee, I. H., and Liu, J. T. (2008). Observation of Internal Tidal Currents in the Kaoping Canyon off Southwestern Taiwan. *Estuarine, Coastal Shelf Sci.* 80, 153–160. doi:10.1016/j.ecss.2008.07.016

Watanabe, T., Kawamura, T., Yamazaki, A., Murayama, M., and Yamano, H. (2014). A 106 Year Monthly Coral Record Reveals that the East Asian Summer Monsoon Modulates winter PDO Variability. *Geophys. Res. Lett.* 41, 3609–3614. doi:10.1002/2014gl060037

Watanabe, T. K., Watanabe, T., Yamazaki, A., Pfeiffer, M., Garbe-Schönberg, D., and Claereboudt, M. R. (2017). Past Summer Upwelling Events in the Gulf of Oman Derived from a Coral Geochemical Record. *Sci. Rep.* 7, 4568. doi:10.1038/s41598-017-04865-5

Wei, G., Mcculloch, M. T., Mortimer, G., Deng, W., and Xie, L. (2009). Evidence for Ocean Acidification in the Great Barrier Reef of Australia. *Geochimica Et Cosmochimica Acta* 73, 2332–2346. doi:10.1016/j.gca.2009.02.009

Xu, B., Bianchi, T. S., Allison, M. A., Dimova, N. T., Wang, H., Zhang, L., et al. (2015). Using Multi-Radiotracer Techniques to Better Understand Sedimentary Dynamics of Reworked Muds in the Changjiang River Estuary and Inner Shelf of East China Sea. *Mar. Geology.* 370, 76–86. doi:10.1016/j.margeo.2015.10.006

Xu, S., Jia, G., Deng, W., Wei, G., Chen, W., and Huh, C.-A. (2014). Carbon Isotopic Disequilibrium between Seawater and Air in the Coastal Northern South China Sea over the Past century. *Estuarine, Coastal Shelf Sci.* 149, 38–45. doi:10.1016/j.ecss.2014.07.008

Conflict of Interest: The authors declare that the research was conducted in the absence of any commercial or financial relationships that could be construed as a potential conflict of interest.

The handling editor declared a past co-authorship with the authors RY and JTL.

Publisher's Note: All claims expressed in this article are solely those of the authors and do not necessarily represent those of their affiliated organizations, or those of the publisher, the editors, and the reviewers. Any product that may be evaluated in this article, or claim that may be made by its manufacturer, is not guaranteed or endorsed by the publisher.